



Published in final edited form as:

J Physiol. 2019 August ; 597(15): 3999–4012. doi:10.1113/JP278119.

The loss of slow skeletal muscle isoform of troponin T in spindle intrafusal fibers explains the pathophysiology of Amish nemaline myopathy

Kentaro Oki¹, Bin Wei¹, Han-Zhong Feng, J.-P. Jin*

Department of Physiology, Wayne State University School of Medicine, Detroit, MI 48201, USA

Abstract

A nonsense mutation at codon Glu180 of *TNNT1* gene causes Amish Nemaline Myopathy (ANM), a recessively inherited disease with infantile lethality. *TNNT1* encodes the slow skeletal muscle isoform of troponin T (ssTnT). The truncated ssTnT is unable to incorporate into myofilament and is degraded in muscle cells. The symptoms of ANM include muscle weakness, atrophy, contracture, and tremors accompanied by clonus. An ssTnT-knockout (KO) mouse model recapitulates key features of ANM such as atrophy of extrafusal slow muscle fibers and increased fatigability. However, the neuromuscular reflex-related symptoms of ANM has not been explained. By isolating muscle spindles from ssTnT-KO and control mice to examine the composition of myofilament proteins, we found that in contrast to extrafusal fibers, intrafusal fibers contain a significant level of cardiac TnT and the low molecular weight splice form of ssTnT. Intrafusal fibers from ssTnT-KO mice have significantly increased cardiac TnT. Rotarod and balance beam tests revealed impaired neuromuscular coordination in ssTnT-KO mice, indicating abnormality in spindle functions. Unlike wild type control, beam running ability of ssTnT-KO mice had blunted response to a spindle sensitizer, succinylcholine. Immunohistochemistry detected ssTnT and cardiac TnT in nuclear bag fibers whereas fast skeletal muscle TnT in nuclear chain fibers and cardiac α -myosin in one of the two nuclear bag fibers. The loss of ssTnT and compensatory increase of cardiac TnT in nuclear bag fibers would increase myofilament Ca^{2+} -sensitivity and tension to affect spindle activities. This mechanism provides an explanation for the pathophysiology of ANM and a novel target for treatment.

Keywords

Amish Nemaline Myopathy; Troponin T Isoforms; Myofilament; Muscle Spindle; Intrafusal Fiber

*Corresponding Author: J.-P. Jin, Department of Physiology, Wayne State University School of Medicine, Detroit, MI 48201, USA. jjin@med.wayne.edu.

Author contributions

KO, BW, JPJ have contributed the conception or design of the work; KO, BW, HZF, JPJ have contributed to the acquisition, analysis or interpretation of data for the work; KO, BW, HZF, JPJ have contributed to drafting the work or revising it critically for important intellectual content; KO, BW, HZF, JPJ approved the final version of the manuscript and agree to be accountable for all aspects of the work in ensuring that questions related to the accuracy or integrity of any part of the work are appropriately investigated and resolved. All persons designated as authors qualify for authorship, and all those who qualify for authorship are listed.

¹These authors contributed equally to this work.

Competing interests

None

Introduction

The contraction of skeletal muscle is activated upon the rise of cytosolic Ca^{2+} via the troponin complex in sarcomeric actin thin filaments (Gordon *et al.*, 2000; Ohtsuki, 2005). Troponin consists of three protein subunits: troponin C (TnC), troponin I (TnI), and troponin T (TnT) that is the tropomyosin-binding and thin filament-anchoring subunit. Troponin T in vertebrates has three muscle type-specific isoforms encoded by homologous genes: *TNNT1* for slow skeletal muscle TnT (ssTnT), *TNNT2* for cardiac TnT (cTnT), and *TNNT3* for fast skeletal muscle TnT (fsTnT). Alternative RNA splicing and post-translational modifications further increase the structural variations of TnT to accommodate the functions of different muscle types (Jin *et al.*, 2008; Wei & Jin, 2016). Cardiac TnT is expressed in embryonic and neonatal skeletal muscles and diminishes during postnatal development (Wang *et al.*, 2001), indicating the functional exchangeability of TnT isoforms. On the other hand, ssTnT is co-expressed with the slow skeletal muscle isoform of TnI in slow-twitch skeletal muscles, demonstrating a physiological pairing of the fiber type-specific isoforms of troponin subunits (Brotto *et al.*, 2006).

A nonsense mutation at codon Glu₁₈₀ in *TNNT1* gene causes Amish Nemaline Myopathy (ANM), a recessively inherited genetic disease with infantile lethality (Johnston *et al.*, 2000). The truncated ssTnT lacks the T2 segment containing the binding sites for TnI, TnC, and one of the tropomyosin-binding sites. It is unable to incorporate into the thin myofilament, resulting in complete loss of ssTnT in ANM muscle cells (Jin *et al.*, 2003; Wang *et al.*, 2005). The symptoms of ANM include muscle weakness, atrophy, contractures, and tremors of the limbs and chin accompanied by sustained clonus (Johnston *et al.*, 2000; Fox *et al.*, 2018). A mouse model of ANM (ssTnT-KO mice) reproduced the complete loss of ssTnT with atrophy of slow-twitch fibers and increased muscle fatigability (Wei *et al.*, 2014). However, it remains unexplained why the loss of only one isoform of TnT results in such severe myopathy whereas ANM muscles contain an abundant physiological level of fsTnT (Jin *et al.*, 2003). Based on its clinical features, ANM was initially considered a neuromuscular disorder (Johnston *et al.*, 2000). Therefore, the possibility that the loss of ssTnT impairs neuromuscular reflex to cause tremors and clonus and augment the myopathy phenotype is worth investigating.

In mammalian skeletal muscles, the muscle spindle is a specialized sensory organ that detects alterations of muscle length by mechanical stretch (Matthews, 1964). Activated by gamma motor neurons, the intrafusal fibers in muscle spindles are contractile to generate a baseline tension that is critical for sensing the length changes (Hulliger, 1984). Each spindle consists of 4–6 intrafusal myofibers that are classified into nuclear bag fibers and nuclear chain fibers based on their morphology and neuronal firing patterns (Hulliger, 1984; Nelson & Hutton, 1985). Unlike extrafusal fibers, embryonic and cardiac isoforms of myosin heavy chain (MHC) are expressed in adult muscle spindles (Maier *et al.*, 1988; Pedrosa *et al.*, 1990; Liu *et al.*, 2005; Osterlund *et al.*, 2012). However, the isoforms of thin filament regulatory proteins in spindle intrafusal fibers have not been characterized.

In the present study, we isolated muscle spindles from wild type (WT) and ssTnT-KO mice to examine the contents of myofilament proteins. We found that normal intrafusal fibers

express high levels of cTnT and an alternatively spliced low molecular weight ssTnT. In the absence of ssTnT, cTnT is significantly increased in spindle intrafusal fibers of ssTnT-KO mice. Rotarod and balance beam tests revealed impaired neuromuscular coordination in ssTnT-KO mice, indicating abnormality of spindle functions. In contrast to WT control, ssTnT-KO mouse's ability of beam running was by low dose treatment of succinylcholine, implicating an effect of the compensatory increase of cTnT on intrafusal fiber contractility and spindle sensitivity. This study lays a groundwork for understanding the pathophysiology of ANM and the development of targeted treatment.

Materials and Methods

Ethical Approval

All animal procedures were approved by the Institutional Animal Care and Use Committee of Wayne State University (Protocol # IACUC-17-12-0437), conducted in accordance with the *Guiding Principles in the Care and Use of Animals* approved by the Council of the American Physiology Society and the principles and standards for reporting animal experiments in *The Journal of Physiology* as described by Grundy (2015).

Animals

Mice were group housed in a 12 h light:12 h dark facility with *ad libitum* access to mouse chow and water. For terminal muscle contractility studies, animals were anesthetized with isoflurane using a small animal anesthesia system (SomnoSuite, Kent Scientific Corp) on a temperature controlled platform. For post mortem procedures and tissue harvesting, euthanasia was performed using cervical dislocation under deep anesthesia.

The *Tnnt1* gene KO mouse line in C57BL/6 background was generated as previously described (Wei *et al.*, 2014). A germline Cre transgene was used to induce loxP-mediated deletion of a genomic segment containing exons 10 to 13 of *Tnnt1* gene. This targeted destruction effectively abolished the expression of ssTnT as validated by the complete loss of ssTnT protein in skeletal muscle, providing an ANM animal model for pathophysiological studies (Wei *et al.*, 2014). Based on PCR genotyping, homozygotes ssTnT-KO mice and WT littermates were used in the present study.

To trace the activity of cTnT gene in spindle intrafusal fibers, we obtained from Prof. Jim Lin at University of Iowa a transgenic mouse line bearing a β -galactosidase reporter under the control of a cloned rat *Tnnt2* gene promoter (Wang *et al.*, 1994; Kracklauer *et al.*, 2013). cTnT^{promoter}-*lacZ*12 mouse line with a high level of transgene expression was used in the present study.

Isolation of mouse spindles

Spindles were isolated from soleus muscles of 3–4 months old mice using a method combining enzymatic digestion and manual microscopic dissection. After the mouse was anesthetized, soleus muscles were dissected from the hindlimbs and transferred to a digestion solution containing 0.2% collagenase I, 2 mM sodium pyruvate, and 0.02% trypsin in high glucose DMEM for incubation at 37°C for 40 min. The muscles were transferred to a

new tube containing fresh digestion solution and incubated at 37°C for another 40 min. The muscles were rinsed with 37°C pre-warmed DMEM and triturated with a wide pore Pasteur pipette to release the individual extrafusal myofibers. Spindles attached with sensory and motor nerves were then manually dissected out of the tissue on a Motic AE30 inverted microscope using a 4X lens. The isolated muscle spindles were removed from the nerve fibers, photographed for morphology evaluation, and pooled for lysis in SDS-gel sample buffer for protein content analysis or fixed and mounted on cover slips for immunofluorescence study.

SDS-PAGE and Western blotting

As described previously (Wei *et al.*, 2014), whole muscle tissue was mechanically homogenized and pooled isolated spindles were directly solubilized in SDS-polyacrylamide gel electrophoresis (PAGE) sample buffer containing 2% SDS and 2% β -mercaptoethanol and heated at 80°C for 3 min. The total protein extracts were resolved on 14% Laemmli gel with an acrylamide to bis-acrylamide ratio of 180:1. The resulting gels were stained with Coomassie Blue R250 or electrically transferred to nitrocellulose membranes at 5 mA/cm² for 15 min using a BioRad semidry transfer apparatus.

After blocking in 1% bovine serum albumin (BSA) in Tris-buffered saline (TBS, 50 mM Tris-Cl, pH 7.6; 150 mM NaCl) containing 0.5% Triton X-100 and 0.05% SDS, the membranes were probed at 4°C with gentle rocking overnight with the following primary antibodies: Anti-cTnT and ssTnT monoclonal antibody (mAb) CT3, anti-fsTnT mAb T12 and anti-TnI mAb TnI-1 (Wei *et al.*, 2014). The membranes were washed with TBS containing 0.5% Triton X-100 and 0.05% SDS to remove excessive primary antibodies and incubated with alkaline phosphatase-conjugated anti-mouse IgG secondary antibody at room temperature for 1 h. Membranes were washed in TBS containing 0.5% Triton X-100 and 0.05% SDS, rinsed in TBS and developed in 5-bromo-4-chloro-3-indolylphosphate–nitro blue tetrazolium substrate solution to visualize the specific protein bands recognized by the primary antibodies. High resolution imaging scans of the membranes were analyzed using NIH ImageJ software to densitometrically quantify the relative levels of the myofibrillar proteins.

Glycerol SDS-PAGE was performed to analyze muscle myosin isoforms (Talmadge & Roy, 1993). Total protein was extracted by homogenizing mouse skeletal muscles or solubilizing isolated spindles in SDS-PAGE sample buffer as above. Samples were resolved on 8% polyacrylamide gels with an acrylamide:bisacrylamide ratio of 50:1 in 30% glycerol, 200 mM Tris base, 100 mM glycine (pH 8.8), and 0.4% SDS. The stacking gel contained 4% polyacrylamide, 70 mM Tris-HCl (pH 6.7), 4 mM EDTA, and 0.4% SDS. The gels were run at 70 V for 24 hours in an icebox, stained with Coomassie Blue R250, and de-stained with 10% acetic acid to detect myosin heavy chain (MHC) bands. Duplicate gels were transferred to nitrocellulose membranes for Western blotting using anti-MHC mAbs FA2 and FA3 as described previously (Jin *et al.*, 1990).

X-Gal staining

X-Gal staining of muscle cryosections was done using a modified method (Ma *et al.*, 2002; Takahashi *et al.*, 2003). Briefly, muscle sections were fixed in ice-cold phosphate-buffered saline (137 mM NaCl, 2.7 mM KCl, 8.1 mM Na₂HPO₄, 1.5 mM KH₂PO₄, PBS) containing 3.7% formaldehyde, 0.5% glutaraldehyde, pH 7.2, at room temperature for 5 min. After washes with PBS for 10 min, the sections were stained with freshly prepared X-Gal solution (1 mg/mL X-Gal in 5 mM K₄Fe(CN)₆·3H₂O and 2 mM MgCl₂) in a humidified box at 37°C overnight. After washing in PBS for 10 min, the stained sections were post-fixed with the fixation solution for 30 min, washed in PBS, mounted with 50% glycerol in PBS, and photographed using a Zeiss Observer 125 microscope (Carl Zeiss AG, Germany).

For X-Gal staining of whole muscle, euthanized mice were perfused with filtered Krebs-Henseleit solution (118 mM NaCl, 25 mM NaHCO₃, 4.7 mM KCl, 1.2 mM KH₂PO₄, 2.25 mM MgSO₄, 2.25 mM CaCl₂, 11 mM D-glucose and oxygenated with 5% CO₂ and 95% O₂ at 37°C and pH 7.4) through cannulation of the left ventricle using a peristaltic pump (Bio-Rad, Hercules, CA) at a flow rate of 6.4 mL/min, followed by fixation perfusion with 3.7% formaldehyde in PBS until the visceral tissues hardened (Kracklauer *et al.*, 2013). The perfusion was then switched back to Krebs-Henseleit solution to wash out excessive formaldehyde before the perfusion of X-Gal solution. After intense color development in the heart, the hindlimb muscles were dissected, rinsed in PBS, post-fixed with 3.7% formaldehyde in PBS at 4°C overnight, whole mounted with 50% glycerol in PBS and photographed using a Zeiss Observer 125 microscope (Carl Zeiss AG, Germany) or cryosectioned for histological examinations (Kracklauer *et al.*, 2013).

Rotarod test

Rotarod testing was used to examine the local neuromuscular reflex function of ssTnT-KO mice. WT and ssTnT-KO mice were first allowed to stay on the stationary rod to acclimate to the environment. Mice were then trained during one session where they were allowed to run forward on a 7 cm diameter rod at the following speeds: 5 rpm (120s), 10 rpm (120s), 15 rpm (60s), linear acceleration from 5 to 15 rpm over 60s, and linear acceleration from 5 to 20 rpm over 60s. Performance at each speed was calculated as the average latency to fall across three trials. Five minutes of rest were given between each trial. As 5 to 15 rpm was determined to be the speed ramp at which the experimental and control groups segregated based on performance, this condition was tested with nine trials over two days with the highest and lowest values removed to obtain the average of the seven remaining values.

Balance beam and succinylcholine sensitivity test

A 12.7 mm square aluminum beam was levelly fixed 50 cm above a table with clamps on metal support stands. Soft padding was placed underneath the beam. A small plastic box was placed at one end of the beam, 80 cm from the starting end. All tests were video-recorded for analysis. Mice were trained to walk across the beam following a protocol similar to one previously established (Luong *et al.*, 2011). The tests were done at baseline and after succinylcholine treatment.

Succinylcholine (SCh) is known as a selective activator of intrafusal muscle fibers (Granit *et al.*, 1953; Taylor *et al.*, 1992; Wang *et al.*, 2012), and it may specifically act on intrafusal bag fibers to evoke spindle discharges (Gladden, 1976). Accordingly, our rationale was that SCh treatment of conscious mice would selectively evoke muscle spindle discharges and affect motor coordination. A change in TnT composition in spindle intrafusal fibers in ssTnT-KO mice would alter the response to SCh treatment.

SCh (VWR, Radnor, PA) was dissolved in 0.9% saline (VetOne, Boise, ID) at 0.1 mg/mL, brought to physiological pH, and filtered to sterilize (0.22 μ m, Millex, Duluth, GA) before being injected subcutaneously (s.c.) into conscious mice. Based on a previous study (Nevins *et al.*, 1993) as well as safety consideration to ensure no incidences of conscious paralysis, a low dose of 0.68 mg/kg, s.c. was determined as the effective treatment in neurologically stimulated *in situ* soleus muscle contractility test (Feng *et al.*, 2009; Wei *et al.*, 2014; Feng and Jin, 2016) and during pilot beam running studies for testing the effect on spindle function in motor coordination.

On a testing day, a baseline beam running test was done 5 min prior to SCh injection with subsequent tests immediately after the injection and every 5 min thereafter until 25 min post-injection when the dose of SCh has been metabolized. Motor performance was assessed by measuring the total time to cross the beam, total time spent moving on the beam, speed while moving, and number of falls.

Immunofluorescence microscopy

Intact spindles and spindle myofibrils isolated from mouse soleus muscle were examined by immunofluorescence microscopy as previously described (Huang *et al.*, 2008). The samples attached on slides were fixed with 50% acetone and 50% methanol for 5 min, blocked with 3% BSA in PBS containing 0.05% Tween-20 (PBS-T), and stained with an anti- α -actinin mouse mAb A7811 (Sigma, clone EA-53), an anti-myosin light chain 2V (MLC2V) rabbit mAb (Abcam), an anti-ssTnT and cTnT mouse mAb CT3, an anti-fsTnT mouse mAb T12, and DAPI for nuclei at 4°C overnight, followed by PBS-T washes and incubation with fluorescein isothiocyanate- or tetramethylrhodamine-conjugated secondary antibody. After final PBS-T washes, fluorescence images were recorded using a Leica spinning disc confocal microscope.

Cryosectioning and immunohistochemistry

Immediately after euthanasia, soleus muscles were rapidly removed from mouse hindlimbs and mounted at their *in vivo* length on a tissue cork, embedded with O.C.T. compound, and snap frozen in pre-chilled (-159°C) 2-methylbutane for 30 s. 5 μ m thick cross sections of the muscle tissues were cut using a Leica CM 1950 cryostat (Buffalo Grove, IL), and serial sections were collected at 200 μ m intervals and mounted on a glass slide to air-dry before storage at -20°C .

Muscle sections were blocked in PBS-T containing 1% BSA at room temperature for 30 min followed with a treatment of 1% H_2O_2 in PBS-T to inactivate endogenous peroxidase. After three 5 min washes with PBS-T, the muscle sections were probed with the anti-thin filament protein antibodies as above or with anti-cardiac α/β -MHC mAb FA2 or anti-cardiac α -MHC

mAb FA3 with gentle rocking at 4°C overnight. The muscle sections were then washed as above and incubated with horseradish peroxidase-conjugated anti-mouse IgG secondary antibody at room temperature for 1 h. The sections were washed again to remove excess secondary antibody, staining of specific myofilament proteins was developed in 3,3-diaminobenzidine-H₂O₂ substrate in a dark box for 30 s and the reaction was terminated by washing with 20 mM Tris-HCl buffer, pH 7.6. After counterstaining of nuclei with haematoxylin, the muscle sections were mounted in 50% glycerol in PBS, sealed using Cytoseal, and photographed using a Zeiss Observer 125 microscope (Carl Zeiss AG, Germany).

Statistical analysis

All quantitative data are presented as mean \pm SEM. Statistical significance was analyzed using Student's *t* test or one-way analysis of variance (ANOVA).

Results

Isolation of spindles from mouse muscles

By histological examination of spindles in serial cross-sectional cryosections of mouse soleus and EDL muscles in 200 μ m intervals, we were able to morphologically identify different sections of a spindle (Figure 1A). With the muscle length maintained at the *in vivo* length, we were able to determine the size of spindle intrafusal fibers in the middle equatorial region as well as in the terminal regions. Each mouse muscle spindle contained 4–5 intrafusal fibers, with 2 nuclear bag fibers and 2–3 nuclear chain fibers.

With combined collagenase I and trypsin digestions followed by manual microscopic dissection, intact individual muscle spindles were successfully isolated with preserved structure with visible equatorial region and flanking intrafusal fibers (Figure 1B).

Identification of myofilament protein isoforms in isolated spindle intrafusal fibers

Using total protein extracted from pooled mouse soleus and EDL muscle spindles, Western blotting identified the myofilament protein isoforms expressed in intrafusal fibers. The spindle intrafusal fibers of adult mice express both ssTnT and cTnT whereas the latter is not expressed in normal adult extrafusal muscle fibers (Figure 2A). Also different from extrafusal fibers, the low molecular weight splice form of ssTnT is predominant in intrafusal fibers at 64.9 \pm 1.1% of total ssTnT while it is only 23.6 \pm 1.5% of total ssTnT in the whole soleus muscle sample (Figure 2B).

Western blots in Figure 2A further showed that the slow skeletal muscle isoform of TnI is predominant in spindle intrafusal fibers at 88.5 \pm 6.5% of total TnI, significantly higher than the 49.3 \pm 2.0% in the total protein extract of adult mouse soleus muscle corresponding to the ~50% slow-twitch fiber content (Figure 2B). While the mouse EDL muscle containing predominantly fast-twitch fibers shows a minimal amount of ssTnT and almost exclusively fast TnI in the total protein extract, ssTnT and slow skeletal muscle isoform of TnI are predominant in spindles isolated from EDL muscle similar to that in soleus muscle spindles (Figure 2A). The results demonstrate that the high abundance of ssTnT and slow skeletal

muscle TnI in intrafusal fibers is an intrinsic feature of spindles from both slow- and fast-twitch muscles, likely critical to the specific contractility of spindle intrafusal fibers uniformly required for normal neuromuscular reflex functions.

The Western blot in Figure 2A also detected significant amounts of cTnT in mouse spindle intrafusal fibers, which is not expressed in normal extrafusal muscle fibers of adult mice. The expression of the cTnT gene in spindle intrafusal fibers was further demonstrated *in situ* in the muscle of cTnT^{promoter}-*lacZ* transgenic mice. X-Gal staining of whole soleus and EDL muscles showed strong activity of cTnT gene promoter specifically in spindle intrafusal fibers with no expression in extrafusal fibers (Figure 3A). X-Gal staining of muscle cross sections showed that the cTnT^{promoter}-*lacZ* reporter gene was active specifically in only 2 of the 5 intrafusal fibers of a spindle (Figure 3B). mAb CT3 immunohistochemistry stain of adjacent cryosections confirmed that cTnT was expressed in the same two intrafusal fibers (Figure 3B). Altogether, biochemical and histological data demonstrate that different from extrafusal muscle fibers, adult mouse spindle constitutively express cTnT in a subset of intrafusal fibers implicating a functional significance.

Much more complex than fast- and slow-twitch extrafusal muscle fibers of adult mice, glycerol SDS-gel revealed multiple MHC variants in intrafusal fibers with similar patterns in spindles from mouse soleus and EDL muscles (Figure 4A). Using mAbs against cardiac MHC isoforms, Western blotting identified that soleus and EDL muscle spindles contain the adult mouse heart-specific α -MHC instead of β -MHC/MHC-I that is predominant in slow-twitch extrafusal skeletal muscle fibers in adult mice (Figure 4B). This finding supports the notion that together with ssTnT and slow skeletal muscle TnI, cTnT and cardiac α -myosin play unique roles in intrafusal fibers to determine the contractile features critical to normal neuromuscular reflex functions.

Expression of slow and cardiac isoforms of myofilament protein in intrafusal fibers with a compensatory increase of cTnT in ssTnT-KO spindles

To investigate the effects of lacking ssTnT in ANM on spindle functions, we examined the TnT isoform contents in intrafusal fibers of ssTnT-KO mice. SDS-gel and mAb CT3 Western blots confirmed the complete loss of ssTnT in total muscle protein extracts of ssTnT-KO mice (Figure 5A). Western blots of isolated spindles showed that in the absence of ssTnT, there is a ~3-fold increase of cTnT, which quantitatively compensated for the loss of ssTnT (Figures 5B & 5C).

On the other hand, ssTnT-KO mouse intrafusal fibers retained slow skeletal muscle TnI as the dominant isoform similar to that in the WT control (Figures 5B & 5D). mAb T12 Western blot in Figure 5B showed similar abundance of fsTnT and similar splice forms in ssTnT-KO and WT muscle spindle intrafusal fibers, of which a low molecular weight splice form is predominant. The mAb CH1 blot also showed similar expression of α -tropomyosin in ssTnT-KO and WT muscle spindle intrafusal fibers (Figure 5B). The mAb FA2 Western blot in the lower panel of Figure 5B further showed similar expression of α -MHC in spindle intrafusal fibers of WT and ssTnT-KO mice.

Impaired coordination of movement of ssTnT-KO mice

To assess the effect of ssTnT deficiency on the ability of mice to coordinate movements, we performed Rotarod test on 2–4 month old age- and sex-matched ssTnT-KO vs. WT mice. After acclimation, tests with accelerating rod rotation detected that ssTnT-KO mice are less capable of maintaining their position on the Rotarod and had a significantly shorter latency to fall when compared to WT controls (Figure 6). The Rotarod protocol was designed with brief testing periods and sufficient rest between trials to prevent fatigue since our previous studies showed that soleus and diaphragm muscles were phenotypically switched to fast fiber dominant with impaired fatigue tolerance (Feng *et al.*, 2009; Wei *et al.*, 2014).

ssTnT-KO mice had a blunted response to low dose succinylcholine treatment

We used a low dose of SCh to selectively activate intrafusal muscle fibers (Granit *et al.*, 1953; Taylor *et al.*, 1992; Wang *et al.*, 2012) to test the effect of altered TnT composition in spindle intrafusal fibers in WT vs. ssTnT-KO mice on motor coordination. Since a previous study indicated that when used at the dose as a muscle relaxant, SCh can desensitize muscle and spindle activations (Nevins *et al.*, 1993), we pre-tested in lightly anesthetized mice and identified a dose of 0.68 mg/kg, s.c., that does not significantly alter neurologically stimulated *in situ* muscle contraction and force-frequency responses of soleus muscle in WT and ssTnT-KO mice (Figure 7A).

This low dose SCh treatment was applied in balance beam test. The baseline ability of beam running before SCh injection confirmed the impairment of coordinated movement of ssTnT-KO mice by a trend for slower speed of moving on the beam in comparison to WT control (Figure 7B). SCh treatment effectively reduced the beam moving speed of WT mice with a plateaued effect 25 min after s.c. injection, consistent with the predicted impairment of neuromuscular coordination (Nevins *et al.*, 1993). However, the SCh treatment did not further decrease the speed of beam running (Figure 7B) or increase the number of falls in ssTnT-KO mice (data not shown). Therefore, despite the impaired baseline spindle function of ssTnT-KO mice, they exhibited a blunted response to low dose SCh stimulation.

No change in overall and sarcomeric structures of ssTnT-KO mouse spindle intrafusal fibers

Isolated muscle spindles from ssTnT-KO mice showed comparable length ($1455.1 \pm 72.8 \mu\text{m}$) to that of WT controls ($1698.6 \pm 135.6 \mu\text{m}$) (Figure 8A & 8B). The total number of spindles counted in serial cross sections of soleus muscle was unchanged in ssTnT-KO mice (7.8 ± 0.3 per muscle vs. 8.3 ± 0.3 per muscle in WT) (Figure 8C). Calculated using α -MHC, ssTnT and cTnT positive areas, the cross sectional size of intrafusal fibers is also similar in ssTnT-KO and WT spindles (Figure 8C).

Immunofluorescence studies of isolated muscle spindles using anti-cTnT/ssTnT mAb CT3 to visualize the striated sarcomere pattern in intrafusal fibers showed that ssTnT-KO did not cause visible changes to myofibril sarcomeric organization as compared with WT control (Figure 8D). This observation was further shown by the normal sarcomere length in ssTnT-KO mouse spindle intrafusal fibers (Figure 8E).

Differential expression of myofilament protein isoforms in different types of intrafusal fibers

Immunofluorescence microscopic imaging of isolated muscle spindles further identified that the cTnT-expressing intrafusal fibers are nuclear bag fibers based on morphological features (Figure 9A) whereas fsTnT expression in intrafusal fibers are exclusively in the nuclear chain fibers (Figure 9A).

Immunohistochemistry studies of serial cross sections of WT mouse soleus muscle detected ssTnT and cTnT specifically in two of the four intrafusal fibers and fsTnT in the other two (Figure 9B). ssTnT-KO spindles retained the same pattern while cTnT quantitatively compensated the loss of ssTnT (Figure 9B). Another interesting finding is that cardiac α -MHC was expressed in only one of the two cTnT/ssTnT expressing intrafusal fibers in both WT and ssTnT-KO mouse muscle spindles (Figure 9B).

These distinct patterns of myofilament protein isoform expression in different intrafusal fibers demonstrate a novel approach to identify the types of intrafusal fibers, which in addition to morphological analysis provides a functional relevance. The preserved expression pattern in ssTnT-KO spindles and the functions of ssTnT/cTnT specifically expressed in nuclear bag fibers (Figure 9A) may indicate a novel target for the treatment of ANM.

Discussion

While extensive studies have shown that the loss of ssTnT in ANM results in loss of slow-twitch extrafusal muscle fibers and reduces the resistance of muscle to fatigue (Feng *et al.*, 2009; Wei *et al.*, 2014), this mechanism alone could not fully explain the severe phenotype of ANM, especially the neuromuscular reflex-related abnormalities such as tremors and clonus (Johnston *et al.*, 2000, Fox *et al.*, 2018). By investigating the myofilament protein isoform contents in spindle intrafusal fibers and the changes in ssTnT-KO mice, the findings of our present study provide the following novel insights into the pathophysiology of ANM and potentially other recessively inherited *TNNT1* myopathies (Amarasinghe *et al.*, 2016; Mondal & Jin, 2016).

Intrafusal and extrafusal myofibers expressed different isoforms and splice forms of TnT

It is known that cTnT is expressed in embryonic, neonatal and actively regenerating skeletal muscles but not in normal adult skeletal muscles. Our finding that cTnT is expressed at significant levels in the intrafusal fibers of normal adult mice (Figures 2A & 3) is intriguing especially with the >3-fold increase in ssTnT-KO mouse spindles when ssTnT is lost.

Alternative RNA splicing of *TNNT1* transcript in the N-terminal region generates high and low molecular weight ssTnT splice forms by inclusion or exclusion of the exon 5-encoded segment. Normal adult mammalian skeletal muscles express mainly the high molecular weight ssTnT (Jin *et al.*, 2000; Larsson *et al.*, 2008). We previously reported that the unique neurological abnormality of type 1 but not type 2 Charcot-Marie-Tooth disease produces a switch of ssTnT to the low molecular weight splice form in extrafusal muscle fibers (Larsson *et al.*, 2008). Comparing with the high molecular weight ssTnT, the low molecular

weight ssTnT with shorter N-terminal variable region has altered molecular conformation and increased binding affinity for tropomyosin and TnI (Larsson *et al.*, 2008).

TnT isoforms with shorter N-terminal variable segments convey lower Ca^{2+} sensitivity as previously studied using chicken fsTnT (Ogut *et al.*, 1999) and human cTnT (Gomes *et al.*, 2002) alternative splice forms. Therefore, the predominant expression of the low molecular weight ssTnT in spindle intrafusal fibers indicates a unique feature of reduced myofilament sensitivity to Ca^{2+} activation that may be critical to maintain a proper tension in intrafusal nuclear bag fibers. On the other hand, the compensatory replacement for the loss of ssTnT by cTnT would produce an abnormally high myofilament Ca^{2+} -sensitivity to generate high tension in intrafusal nuclear bag fibers and increase spindle's sensitivity to length changes and stretch as seen with the symptoms of tremors and clonus in ANM patients (Johnston *et al.*, 2000, Fox *et al.*, 2018). Supporting this hypothesis, a previous study has demonstrated that replacement of cTnT in skinned porcine ventricular papillary muscle fibers with ssTnT decreased in the Ca^{2+} sensitivity of force development (Pinto *et al.*, 2012).

Expression of cardiac α -myosin in spindle intrafusal fibers

While the extrafusal fibers of slow-twitch skeletal muscles and cardiomyocytes share a common myosin isoform (named MHC-I in skeletal muscle and β -MHC in cardiac muscle), cardiac α -MHC but not the slow skeletal muscle type of β -MHC is expressed in spindle intrafusal fibers of adult mice (Figure 4). This finding is consistent with the previously reported cardiac α -MHC expression in human and rabbit spindle intrafusal fibers (Pedrosa *et al.*, 1990).

In addition to the presence of multiple other isoforms of myosin in mouse spindle intrafusal fibers, α -MHC is the most abundant isoform (Figure 4A). It is known that α -MHC has a much faster ATPase rate than that of β -MHC (Morano, 1999), implying the need of faster contractile velocity and/or stronger force in intrafusal fibers for the function of muscle spindles. Further suggesting a unique role of α -MHC in spindle functions, we found that α -MHC is present in only one of the two ssTnT/cTnT expressing intrafusal nuclear bag fibers (Figure 9), of which the specific functional impact merits further investigation.

ssTnT-KO mice have structurally preserved spindles but impaired neuromuscular coordination

We have previously reported that in ssTnT-KO mice, extrafusal slow-twitch muscle fibers were severely atrophic due to the loss of ssTnT. However, the loss of ssTnT in spindle intrafusal fibers did not lead to atrophy or degeneration of the two ssTnT expressing nuclear bag fibers (Figure 9), and normal overall and sarcomere structures of the spindle were also retained (Figure 8). This difference between extrafusal and intrafusal fibers of ssTnT-KO mice is presumably due to effective compensation of total amount of TnT protein by the upregulation of cTnT in intrafusal but not extrafusal fibers (Figure 5).

ANM was initially considered a neurological disorder (Johnston *et al.*, 2000), and this notion is validated in our present study. The more detailed ANM phenotypes and clinical history which we recently reported as a summary from around 100 cases (Fox *et al.*, 2018) documented tremors of the limbs and chin accompanied by sustained clonus. A single

stretch of muscle can trigger this symptom, indicating a primary abnormality in monosynaptic stretch reflex. Although ssTnT-KO mice did not present obvious tremors, their preserved spindle structures and upregulation of cTnT in spindle intrafusal fibers do not fully compensate for the loss of ssTnT function in neuromuscular reflex-related activities as shown by the impaired coordination of movements in Rotarod and balance beam tests (Figures 6 & 7B).

Our present study demonstrated a major functional difference between ssTnT and cTnT despite their functional exchangeability. The data suggest that the loss of ssTnT and compensatory upregulation of cTnT in intrafusal nuclear bag fibers may be an underlying mechanism of the neuromuscular reflex-related functional abnormality by increasing spindle's intrinsic tension and sensitivity in responding to changes in muscle length and stretch due to increased myofilament Ca²⁺-sensitivity.

Pathophysiologic and therapeutic implications of the compensation for loss of ssTnT by cTnT in ANM spindle intrafusal fibers

We have previously reported that the loss of ssTnT leads to severe atrophy of extrafusal slow-twitch fibers and was not accompanied by compensation of other TnT isoforms (Feng *et al.*, 2009; Wei *et al.*, 2014). We now found that cTnT coexists with ssTnT in normal spindle intrafusal nuclear bag fibers and is effectively upregulated to fully restore the normal level of total TnT in intrafusal myofilaments (Figure 5). ssTnT KO results in diminished ssTnI in slow twitch muscle as a result of fast-switch of extrafusal fiber types (Wei *et al.*, 2014). However, the spindle intrafusal fibers of *Tnnt1* KO mice remain to contain predominantly ssTnI (Figure 5B and 5D), which may be a protective benefit of the compensatory upregulation of cTnT in the intrafusal but not extrafusal muscle fibers of ssTnT-KO mice.

Despite the preserved TnI, tropomyosin and MHC contents (Figure 5), the TnT isoform swap in ssTnT-KO mice may potentially alter myofilament Ca²⁺-sensitivity and tension in the spindle intrafusal fibers as demonstrated previous studies (Ogut *et al.*, 1999; Gomes *et al.*, 2002; Pinto *et al.*, 2012). cTnT conveys higher myofilament Ca²⁺ sensitivity than that by ssTnT, especially the low molecular weight splice form of ssTnT present in normal intrafusal fibers. Therefore, abnormal increase in Ca²⁺ sensitivity of myofilaments to produce higher tension in the nuclear bag fibers corresponding to higher spindle sensitivity to length change and stretch due to substitution for the loss of ssTnT by cTnT may be responsible for the blunted response to SCh that may specifically act on intrafusal bag fibers to evoke spindle discharges (Gladden, 1976) (Figure 7B) and the tremors and clonus of ANM patients (Johnston *et al.*, 2000; Fox *et al.*, 2018).

It is worth noting that the truncated ANM ssTnT is unable to incorporate into myofilaments (Wang *et al.*, 2005) and non-myofilament-associated ssTnT fragments are cytotoxic and induce apoptosis (Jeong *et al.*, 2009). The ssTnT mutation-originated pathogenesis and pathophysiology of ANM may also be complicated by other non-canonical effects involving proteolytic fragmentation of TnT and TnT translocation into the nuclei as reported in previous studies (Zhang *et al.*, 2015; Johnston *et al.*, 2017; Zhang *et al.*, 2016; Pinto *et al.*, 2017). Future studies are merited to investigate whether such non-contractile functions of the

mutant ssTnT could at least conditionally worsen the phenotypes of ANM by causing apoptosis of spindle intrafusal muscle cells.

As a therapeutic implication, the upregulation of cTnT in ssTnT-KO mouse intrafusal fibers completely compensates for the amount of total TnT in the myofibrils. With functional exchangeability between the two TnT isoforms, this compensation not only fully preserves spindle structure and basal activities but also lays a critical foundation and identifies a molecular target for the treatment of ANM by functional manipulations at the myofilament level, especially cTnT function and Ca²⁺-sensitivity in spindle intrafusal fibers.

Acknowledgements

We thank Prof. Jim Lin for providing the cTnT^{Promoter}-lacZ transgenic mice.

Funding

This work was supported by grants from the National Institutes of Health (HL127691 and 138007 to JPJ).

References

- Amarasinghe C, Hossain MM & Jin JP. (2016). Functional Basis of Three New Recessive Mutations of Slow Skeletal Muscle Troponin T Found in Non-Amish TNNT1 Nemaline Myopathies. *Biochemistry* 55, 4560–4567. [PubMed: 27429059]
- Brotto MA, Biesiadecki BJ, Brotto LS, Nosek TM & Jin JP. (2006). Coupled expression of troponin T and troponin I isoforms in single skeletal muscle fibers correlates with contractility. *Am J Physiol Cell Physiol* 290, C567–576. [PubMed: 16192301]
- Feng HZ, Wei B & Jin JP. (2009). Deletion of a genomic segment containing the cardiac troponin I gene knocks down expression of the slow troponin T gene and impairs fatigue tolerance of diaphragm muscle. *J Biol Chem* 284, 31798–31806. [PubMed: 19797054]
- Feng HF & Jin JP. (2016) Carbonic Anhydrase III Plays an Anti-Fatigue Role in Skeletal Muscle. *Frontiers in Striated Muscle Physiology* 7, 597.
- Fox MD, Carson VJ, Feng HZ, Lawlor MW, Gray JT, Brigatti KW, Jin JP & Strauss KA. (2018). TNNT1 nemaline myopathy: natural history and therapeutic frontier. *Hum Mol Genet* 27, 3272–3282. [PubMed: 29931346]
- Gladden MH. (1976). Structural features relative to the function of intrafusal muscle fibres in the cat. *Prog Brain Res* 44, 51–59. [PubMed: 137428]
- Gomes AV, Guzman G, Zhao J, & Potter JD. (2002) Cardiac troponin T isoforms affect the Ca²⁺ sensitivity and inhibition of force development. Insights into the role of troponin T isoforms in the heart. *J Biol Chem* 277, 35341–35349. [PubMed: 12093807]
- Gordon AM, Homsher E & Regnier M. (2000). Regulation of contraction in striated muscle. *Physiol Rev* 80, 853–924. [PubMed: 10747208]
- Granit R, Skoglund S & Thesleff S. (1953). Activation of muscle spindles by succinylcholine and decamethonium, the effects of curare. *Acta Physiol Scand* 28, 134–151. [PubMed: 13079899]
- Grundy D (2015) Principles and standards for reporting animal experiments in *The Journal of Physiology and Experimental Physiology J Physiol*, 593, 2547–2549. [PubMed: 26095019]
- Huang QQ, Feng HZ, Liu J, Du J, Stull LB, Moravec CS, Huang X & Jin JP. (2008). Co-expression of skeletal and cardiac troponin T decreases mouse cardiac function. *Am J Physiol Cell Physiol* 294, C213–222. [PubMed: 17959729]
- Hulliger M (1984). The mammalian muscle spindle and its central control. *Rev Physiol Biochem Pharmacol* 101, 1–110. [PubMed: 6240757]
- Jeong E, Wang X, Xu K, Hossain MM & Jin JP. (2009) Non-myofilament-associated troponin T fragments induce apoptosis. *Am. J. Physiol:Heart Circ Physiol* 297, H283–92. [PubMed: 19395545]

- Jin JP, Brotto MA, Hossain MM, Huang QQ, Brotto LS, Nosek TM, Morton DH & Crawford TO. (2003). Truncation by Glu180 nonsense mutation results in complete loss of slow skeletal muscle troponin T in a lethal nemaline myopathy. *J Biol Chem* 278, 26159–26165. [PubMed: 12732643]
- Jin JP, Chen A, Ogut O & Huang QQ. (2000). Conformational modulation of slow skeletal muscle troponin T by an NH(2)-terminal metal-binding extension. *Am J Physiol Cell Physiol* 279, C1067–1077. [PubMed: 11003587]
- Jin JP, Malik ML & Lin JJ. (1990). Monoclonal antibodies against cardiac myosin heavy chain. *Hybridoma* 9, 597–608. [PubMed: 1706314]
- Jin JP, Zhang Z & Bautista JA. (2008). Isoform diversity, regulation, and functional adaptation of troponin and calponin. *Crit Rev Eukaryot Gene Expr* 18, 93–124. [PubMed: 18304026]
- Johnston JJ, Kelley RI, Crawford TO, Morton DH, Agarwala R, Koch T, Schaffer AA, Francomano CA & Biesecker LG. (2000) A novel nemaline myopathy in the Amish caused by a mutation in troponin T1. *Am J Hum Genet* 67, 814–821. [PubMed: 10952871]
- Johnston JR, Chase PB, Pinto JR. (2017) Troponin through the looking-glass: emerging roles beyond regulation of striated muscle contraction. *Oncotarget* 9, 1461–1482. [PubMed: 29416706]
- Kracklauer MP, Feng HZ, Jiang W, Lin JL, Lin JJ & Jin JP. (2013). Discontinuous thoracic venous cardiomyocytes and heart exhibit synchronized developmental switch of troponin isoforms. *FEBS J* 280, 880–891. [PubMed: 23176202]
- Larsson L, Wang X, Yu F, Hook P, Borg K, Chong SM & Jin JP. (2008). Adaptation by alternative RNA splicing of slow troponin T isoforms in type 1 but not type 2 Charcot-Marie-Tooth disease. *Am J Physiol Cell Physiol* 295, C722–731. [PubMed: 18579801]
- Liu JX, Eriksson PO, Thornell LE & Pedrosa-Domellof F. (2005). Fiber content and myosin heavy chain composition of muscle spindles in aged human biceps brachii. *J Histochem Cytochem* 53, 445–454. [PubMed: 15805419]
- Luong TN, Carlisle HJ, Southwell A & Patterson PH. (2011). Assessment of motor balance and coordination in mice using the balance beam. *J Vis Exp*
- Ma W, Rogers K, Zbar B & Schmidt L. (2002). Effects of different fixatives on beta-galactosidase activity. *J Histochem Cytochem* 50, 1421–1424. [PubMed: 12364575]
- Maier A, Gambke B & Pette D. (1988). Immunohistochemical demonstration of embryonic myosin heavy chains in adult mammalian intrafusal fibers. *Histochemistry* 88, 267–271. [PubMed: 2966785]
- Matthews PB. (1964). Muscle Spindles and Their Motor Control. *Physiol Rev* 44, 219–288. [PubMed: 14152906]
- Mondal A & Jin JP. (2016). Protein Structure-Function Relationship at Work: Learning from Myopathy Mutations of the Slow Skeletal Muscle Isoform of Troponin T. *Front Physiol* 7, 449. [PubMed: 27790152]
- Morano I (1999). Tuning the human heart molecular motors by myosin light chains. *J Mol Med (Berl)* 77, 544–555. [PubMed: 10494800]
- Nelson DL & Hutton RS. (1985). Dynamic and static stretch responses in muscle spindle receptors in fatigued muscle. *Med Sci Sports Exerc* 17, 445–450. [PubMed: 3162075]
- Nevins ME, Nash SA & Beardsley PM. (1993). Quantitative grip strength assessment as a means of evaluating muscle relaxation in mice. *Psychopharmacology (Berl)* 110, 92–96. [PubMed: 7870904]
- Ogut O, Granzier H & Jin JP. (1999). Acidic and basic troponin T isoforms in mature fast-twitch skeletal muscle and effect on contractility. *Am J Physiol* 276, C1162–1170. [PubMed: 10329966]
- Ohtsuki I (2005). Molecular basis of calcium regulation of striated muscle contraction. *Adv Exp Med Biol* 565, 223–231. [PubMed: 16106978]
- Osterlund C, Lindstrom M, Thornell LE & Eriksson PO. (2012). Remarkable heterogeneity in myosin heavy-chain composition of the human young masseter compared with young biceps brachii. *Histochem Cell Biol* 138, 669–682. [PubMed: 22777345]
- Pedrosa F, Soukup T & Thornell LE. (1990). Expression of an alpha cardiac-like myosin heavy chain in muscle spindle fibres. *Histochemistry* 95, 105–113. [PubMed: 2150514]

- Pinto JR, Gomes AV, Jones MA, Liang J, Nguyen S, Miller T, Parvatiyar MS, & Potter JD. (2012) The functional properties of human slow skeletal troponin T isoforms in cardiac muscle regulation. *J Biol Chem* 287, 37362–37370. [PubMed: 22977240]
- Pinto JR, Muller-Delp J, Chase PB. (2017) Will you still need me (Ca²⁺, TnT, and DHPR), will you still cleave me (calpain), when I'm 64? *Aging Cell* 16, 202–204. [PubMed: 28008709]
- Takahashi M, Hakamata Y, Takeuchi K & Kobayashi E. (2003). Effects of different fixatives on beta-galactosidase activity. *J Histochem Cytochem* 51, 553–554. [PubMed: 12710460]
- Talmadge RJ & Roy RR. (1993). Electrophoretic separation of rat skeletal muscle myosin heavy-chain isoforms. *J Appl Physiol* (1985) 75, 2337–2340. [PubMed: 8307894]
- Taylor A, Durbaba R & Rodgers JF. (1992). The classification of afferents from muscle spindles of the jaw-closing muscles of the cat. *J Physiol* 456, 609–628. [PubMed: 1293289]
- Wang J, Jones C, Norcross M, Bohnlein E & Razzaque A. (1994). Identification and characterization of a human herpesvirus 6 gene segment capable of transactivating the human immunodeficiency virus type 1 long terminal repeat in an Sp1 binding site-dependent manner. *J Virol* 68, 1706–1713. [PubMed: 8107231]
- Wang Q, Reiter RS, Huang QQ, Jin JP & Lin JJ. (2001). Comparative studies on the expression patterns of three troponin T genes during mouse development. *Anat Rec* 263, 72–84. [PubMed: 11331973]
- Wang X, Huang QQ, Breckenridge MT, Chen A, Crawford TO, Morton DH & Jin JP. (2005). Cellular fate of truncated slow skeletal muscle troponin T produced by Glu180 nonsense mutation in amish nemaline myopathy. *J Biol Chem* 280, 13241–13249. [PubMed: 15665378]
- Wang Z, Li L & Frank E. (2012). The role of muscle spindles in the development of the monosynaptic stretch reflex. *J Neurophysiol* 108, 83–90. [PubMed: 22490553]
- Wei B & Jin JP. (2016). TNNT1, TNNT2, and TNNT3: Isoform genes, regulation, and structure-function relationships. *Gene* 582, 1–13. [PubMed: 26774798]
- Wei B, Lu Y & Jin JP. (2014). Deficiency of slow skeletal muscle troponin T causes atrophy of type I slow fibres and decreases tolerance to fatigue. *J Physiol* 592, 1367–1380. [PubMed: 24445317]
- Zhang T, Pereyra AS, Wang ZM, Birbrair A, Reisz JA, Files DC, Purcell L, Feng X, Messi ML, Feng H, Chalovich J, Jin JP, Furdul C, Delbono O. (2016) Calpain inhibition rescues troponin T3 fragmentation, increases Cav1.1, and enhances skeletal muscle force in aging sedentary mice. *Aging Cell* 15, 488–498. [PubMed: 26892246]
- Zhang T, Taylor J, Jiang Y, Pereyra AS, Messi ML, Wang ZM, Hereñú C, Delbono O. (2015) Troponin T3 regulates nuclear localization of the calcium channel Cav β 1a subunit in skeletal muscle. *Exp Cell Res* 336, 276–286. [PubMed: 25981458]

Key point summaries

- The pathogenic mechanism and neuromuscular reflex-related phenotype such as tremors and clonus of Amish Nemaline Myopathy and other recessively inherited *TNNT1* myopathies are not fully understood.
- The truncated slow skeletal muscle isoform of troponin T (ssTnT) encoded by the mutant *TNNT1* gene is unable to incorporate into myofilament and is degraded in muscle cells.
- Different from that in extrafusal muscle fibers, spindle intrafusal fibers of normal mice contain a significant level of cardiac TnT and the low molecular weight splice form of ssTnT. Intrafusal fibers of ssTnT-knockout mice have significantly increased cardiac TnT.
- Rotarod and balance beam tests revealed abnormal neuromuscular coordination in ssTnT-knockout mice and blunted response to a spindle sensitizer, succinylcholine.
- The loss of ssTnT and compensatory increase of cardiac TnT in intrafusal nuclear bag fibers may increase myofilament Ca^{2+} -sensitivity and tension to impair spindle function, identifying a novel mechanism for the development of targeted treatment.

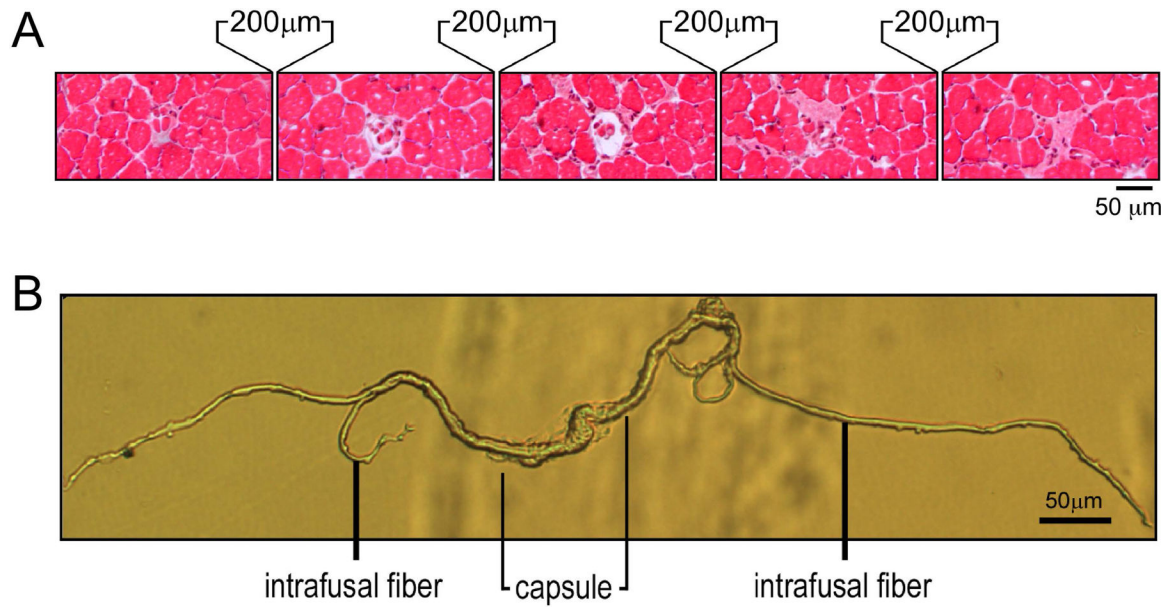


Figure 1. Identification and isolation of mouse muscle spindles.

A. Serial cross sections of a mouse soleus muscle at 200 μm intervals revealed both the central capsule and intrafusal myofibers of a muscle spindle. B. A muscle spindle isolated from mouse soleus muscle using enzymatic digestion and micro-dissection showing the central capsule and intrafusal myofibers.

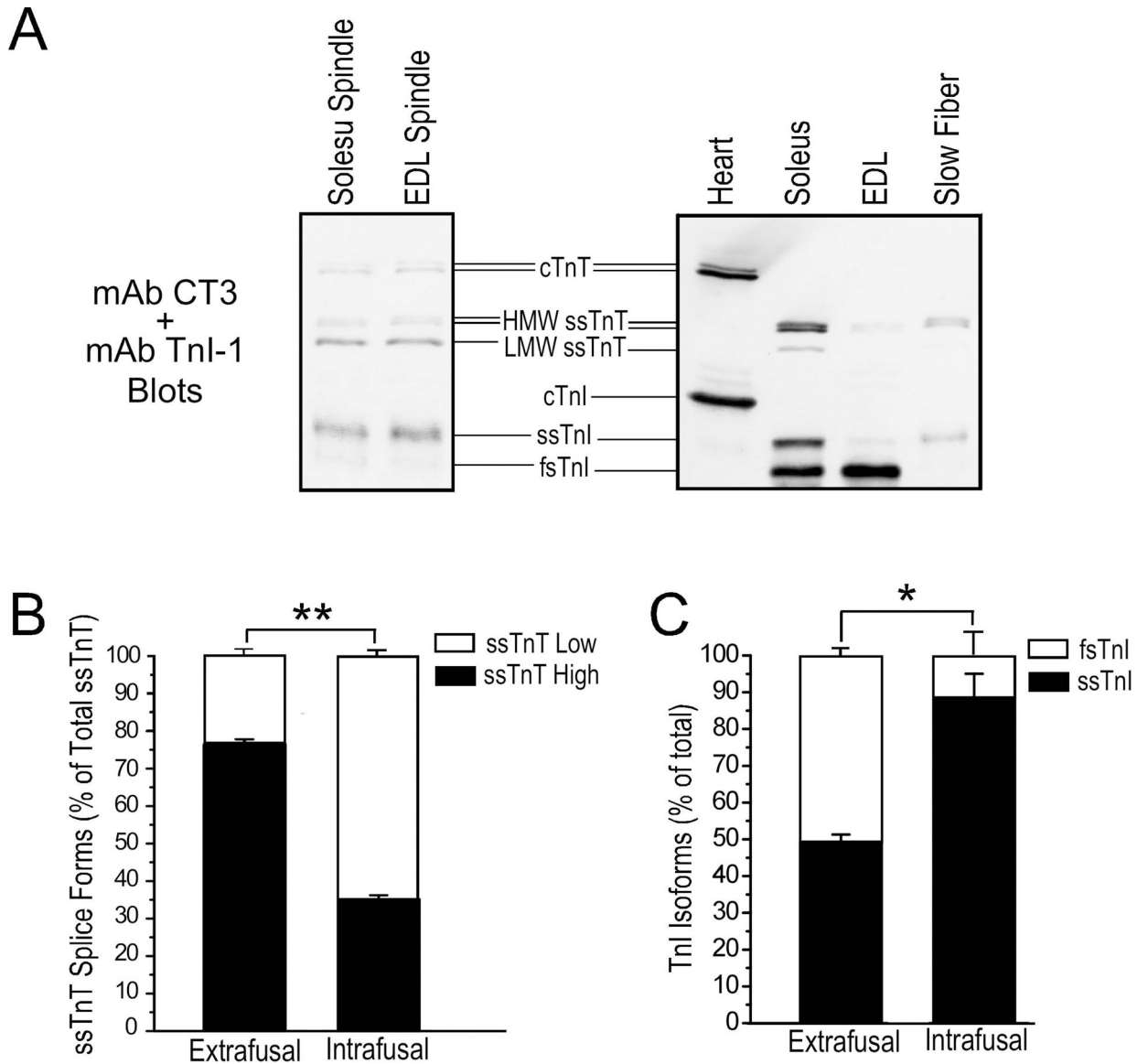


Figure 2. Intrafusal fibers have different thin myofilament protein contents from that in extrafusal fibers.

A. The representative TnT and TnI Western blots in the left panel show that ssTnT is expressed at significant levels in spindle intrafusal fibers of WT mouse with the low molecular weight splice form predominant. cTnT is also expressed in adult mouse muscle spindle intrafusal fibers. Slow skeletal muscle TnI was the major TnI isoform in muscle spindles. Total protein extracts from adult mouse cardiac, slow and fast muscles are shown as controls in the right panel. B & C. Densitometry quantification of the Western blots demonstrate the significantly different ssTnT splice form and TnI isoform contents of isolated intrafusal fibers and total muscle protein extracts representing extrafusal fibers. * $P < 0.05$; ** $P < 0.001$.

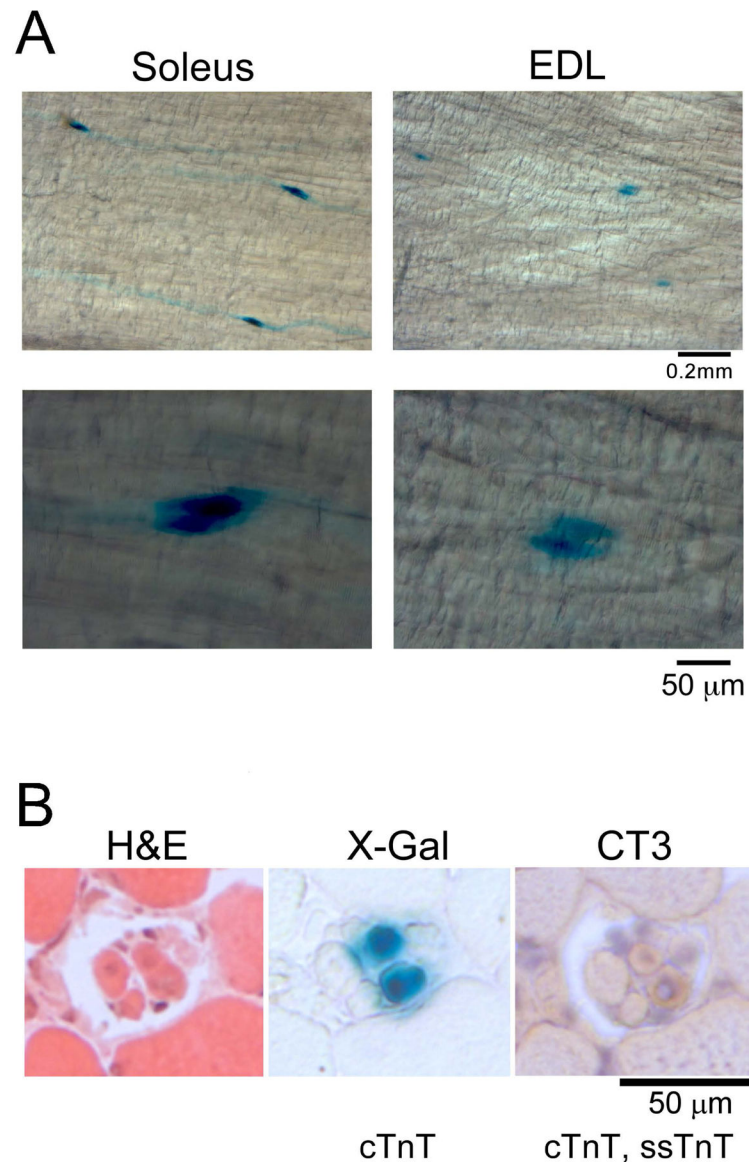


Figure 3. Active cTnT gene expression in spindle intrafusal fibers of adult mice.

A. X-Gal whole muscle staining in transgenic mice expressing a cTnT^{promoter}-driven *lacZ* reporter gene confirmed active expression of cTnT gene in intrafusal fibers of adult mouse muscle spindles. B. Serial cross sections of cTnT^{promoter}-LacZ mouse soleus muscle showed cTnT gene expression in two of the four spindle intrafusal fibers.

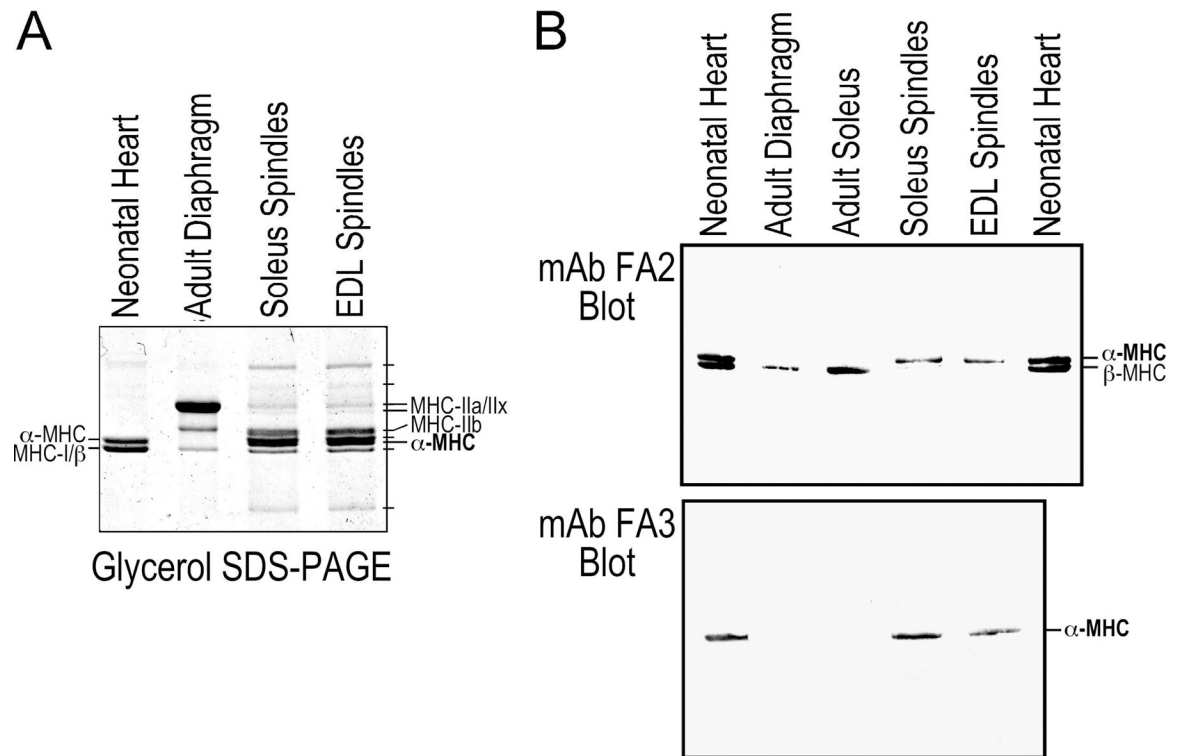


Figure 4. Myosin isoforms in spindle intrafusal fibers.

A. The glycerol SDS-PAGE showed isoforms of myosin heavy chain (MHC) in muscle spindles isolated from soleus and EDL muscles. Significantly different from the adult diaphragm control that contains all four adult skeletal muscle MHC isoforms, cardiac α -MHC is a major component in intrafusal fibers together with skeletal muscle MHC IIa, IIx, IIb and several other unique MHC variants. B. mAb FA2 and FA3 Western blots confirmed that spindle intrafusal fibers of adult mouse soleus and EDL muscles express only cardiac α -MHC whereas β -MHC (MHC-I) is expressed in extrafusal fibers of slow-twitch muscles.

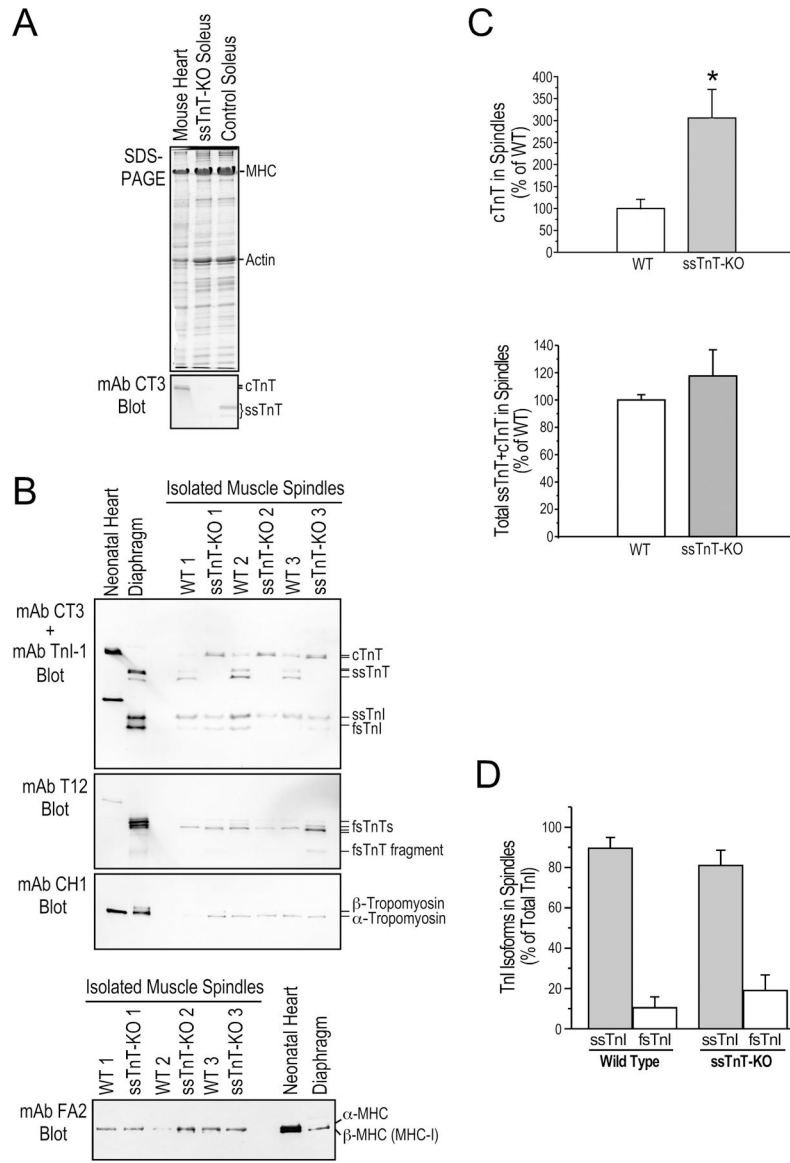


Figure 5. Altered myofilament protein contents in ssTnT-KO mouse spindle intrafusal fibers. A. SDS-gel and mAb CT3 Western blot demonstrate the complete loss of ssTnT in *Tnnt1*-KO mouse soleus muscle with a detectable expression of cTnT reflecting the active regeneration (Wei *et al.*, 2014). Normal mouse heart and soleus muscle were used as controls. B. Western blots of muscle spindle protein extracts from 3 WT and 3 ssTnT-KO mice using a mixture of mAbs CT3 and Tnl-1 demonstrated significantly increased level of cTnT in the intrafusal fibers of ssTnT-KO mice while slow skeletal muscle Tnl (ssTnl) remains the major form in the intrafusal fibers. mAb T12 blot detected a low molecular weight splice form as the major fsTnT in the intrafusal fibers of both WT and ssTnT-KO mice. mAb CH1 blot showed α -tropomyosin in the intrafusal fibers of both WT and ssTnT-KO mice. Neonatal mouse heart and adult diaphragm protein extracts were used as controls. The mAb FA2 Western blot in the lower panel showed no significant change in cardiac MHC isoform contents in ssTnT-KO spindle intrafusal fibers. C. Densitometry analysis

quantified the significant increase of cTnT in ssTnT-KO muscle spindle intrafusal fibers, which completely compensated for the loss of ssTnT to produce a normal level of total cTnT +ssTnT comparable to WT controls. D. α Densitometry quantification confirmed that ssTnI remains the predominant isoform in ssTnT-KO muscle spindle intrafusal fibers. *P<0.05.

Author Manuscript

Author Manuscript

Author Manuscript

Author Manuscript

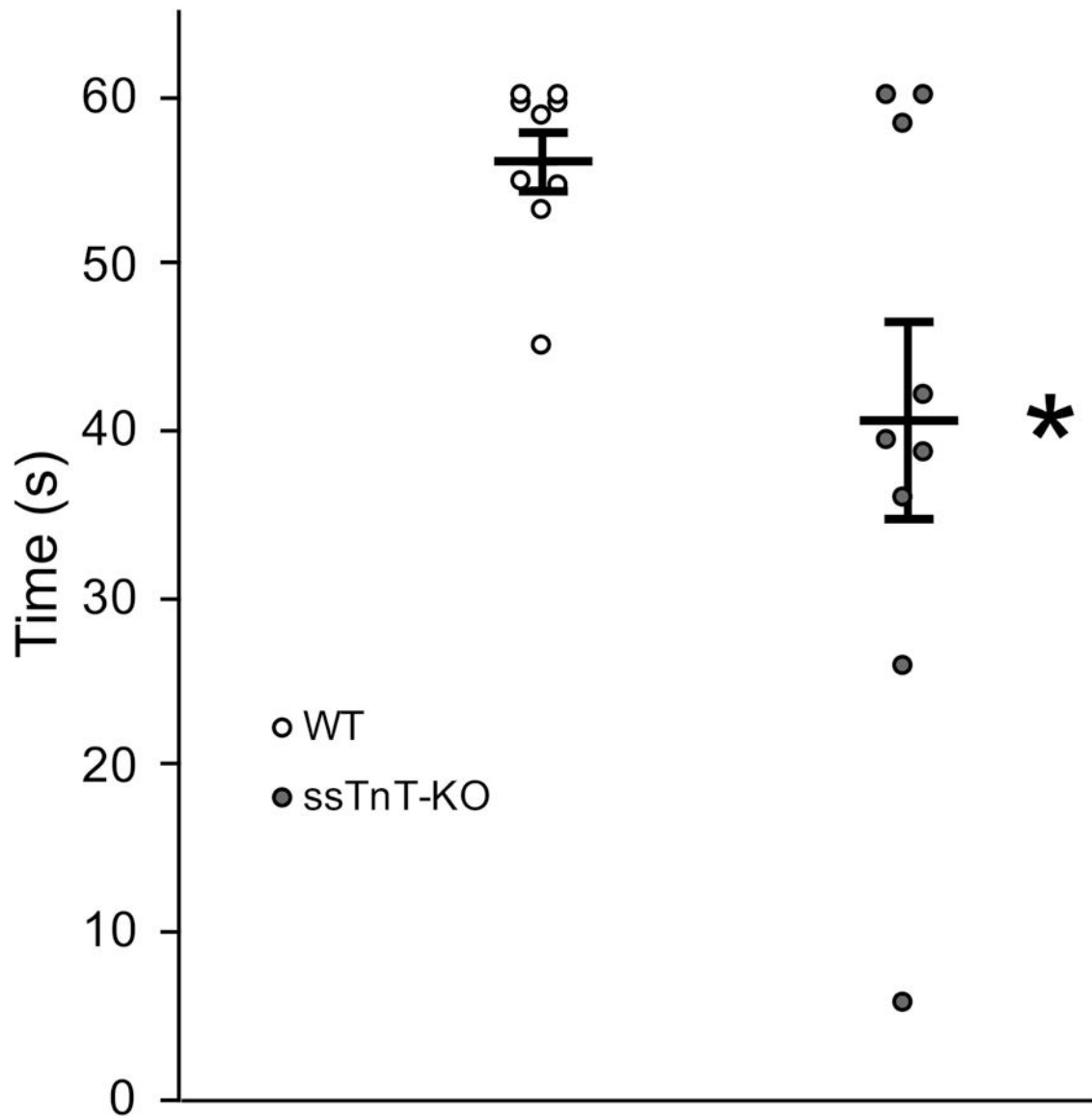


Figure 6. ssTnT-KO affects proprioceptive function in mice.

Rotarod test found that while all WT mice are generally capable of maintaining position on Rotarod during the protocol, a majority of ssTnT-KO mice are incapable of maintaining their position on the Rotarod for more than 45 seconds. Quantitative analysis showed that the average length of time maintaining position on the Rotarod was significantly shorter in ssTnT-KO mice relative to WT control (* $P < 0.05$ in one-way ANOVA, $n = 9$ mice in each group).

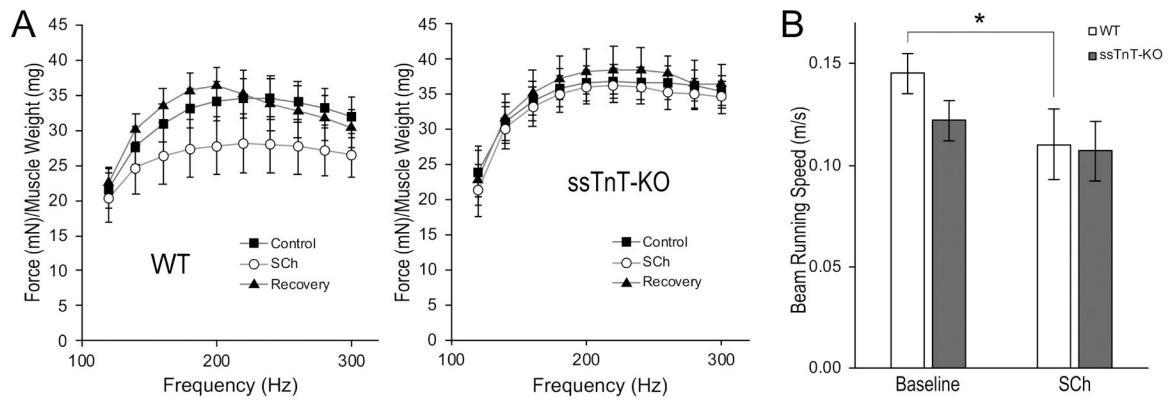


Figure 7. ssTnT-KO mice showed a blunted response to low dose of succinylcholine treatment.

A. Succinylcholine (SCh) 0.68 mg/kg administered s.c. to lightly anesthetized mice during neurologically stimulated *in situ* soleus muscle contractions did not significantly alter force production during the force-frequency response test. The Control curve is the force-frequency relationship measured before SCh treatment. The Recovery curve was recorded 40 minutes after SCh injection, at which the drug should have been metabolized. The trends were not different between WT and ssTnT-KO mice, indicating that the low dose SCh treatment does not significantly alter muscle contractility. B. The low dose SCh treatment in conscious mice during balance beam tests significantly decreased the average running speed in WT mice, consistent with the established pharmacologic effect of SCh on spindle sensitivity and neuromuscular reflex coordinated movement. The average beam running speed of ssTnT-KO mice was slower than that of WT mice at the baseline, consistent with the defective coordination of movement shown in Rotarod test, which however was not significantly affected by the low dose SCh treatment. * $P < 0.05$ by RM ANOVA, $n = 8$ mice in each group.

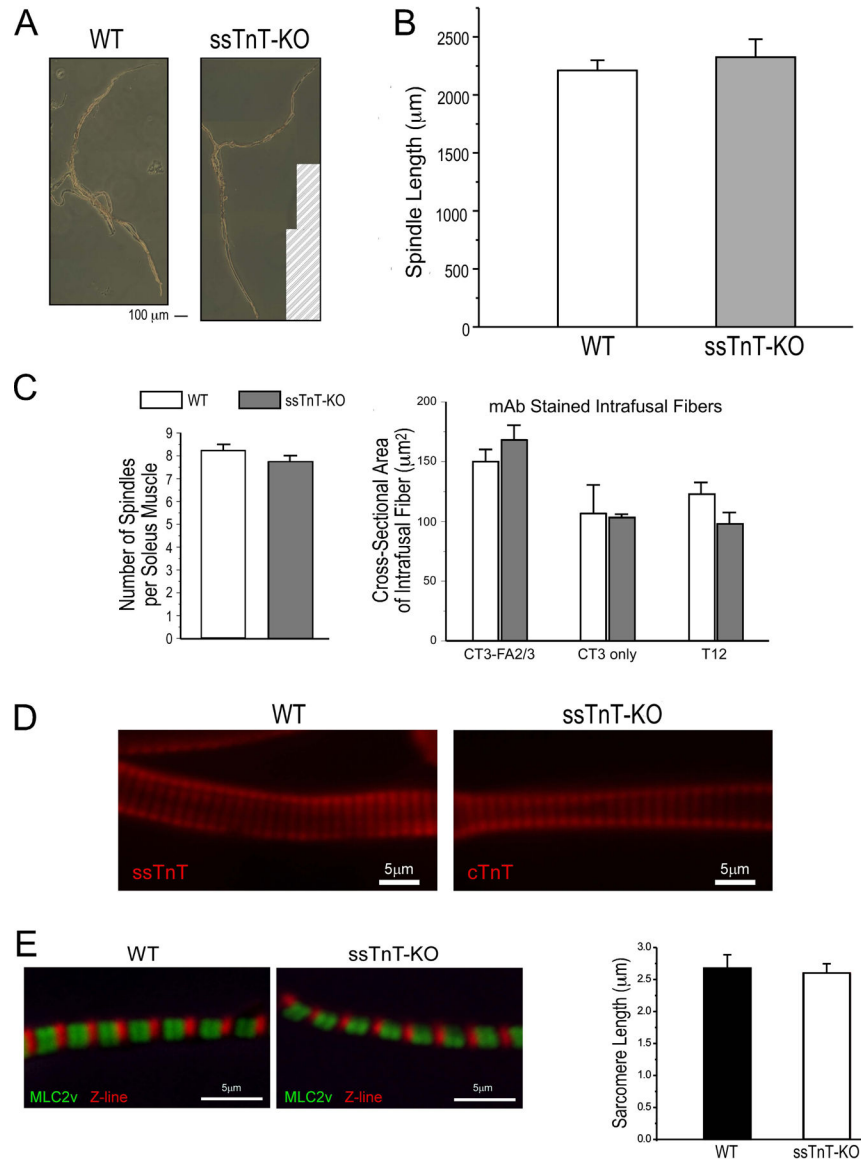


Figure 8. Preserved structure of muscle spindles in ssTnT-KO mice.

A. The representative images show similar morphology of spindles isolated from soleus muscles of WT and ssTnT-KO mice in the presence of 10 mM BDM that inhibited myosin motor activity. The images were composited from multiple photographs in order to cover the whole spindles and the hatch-lined area in the ssTnT-KO panel did not have original photographs. B. The overall length of spindles isolated from ssTnT-KO soleus muscles were same as that from WT mice. C. Quantified in immunohistologically stained muscle cross sections, ssTnT-KO and WT mouse soleus muscles had similar numbers of spindles and similar sizes of various intrafusal fibers. D Immunofluorescence images showed normal striated myofibrils in nuclear bag fibers from a ssTnT-KO mouse spindle as compared with the WT control. E. Immunofluorescence staining of isolated myofibrils showed preserved sarcomere structure and normal resting sarcomere length in ssTnT-KO spindle nuclear bag fibers as compared with WT controls.

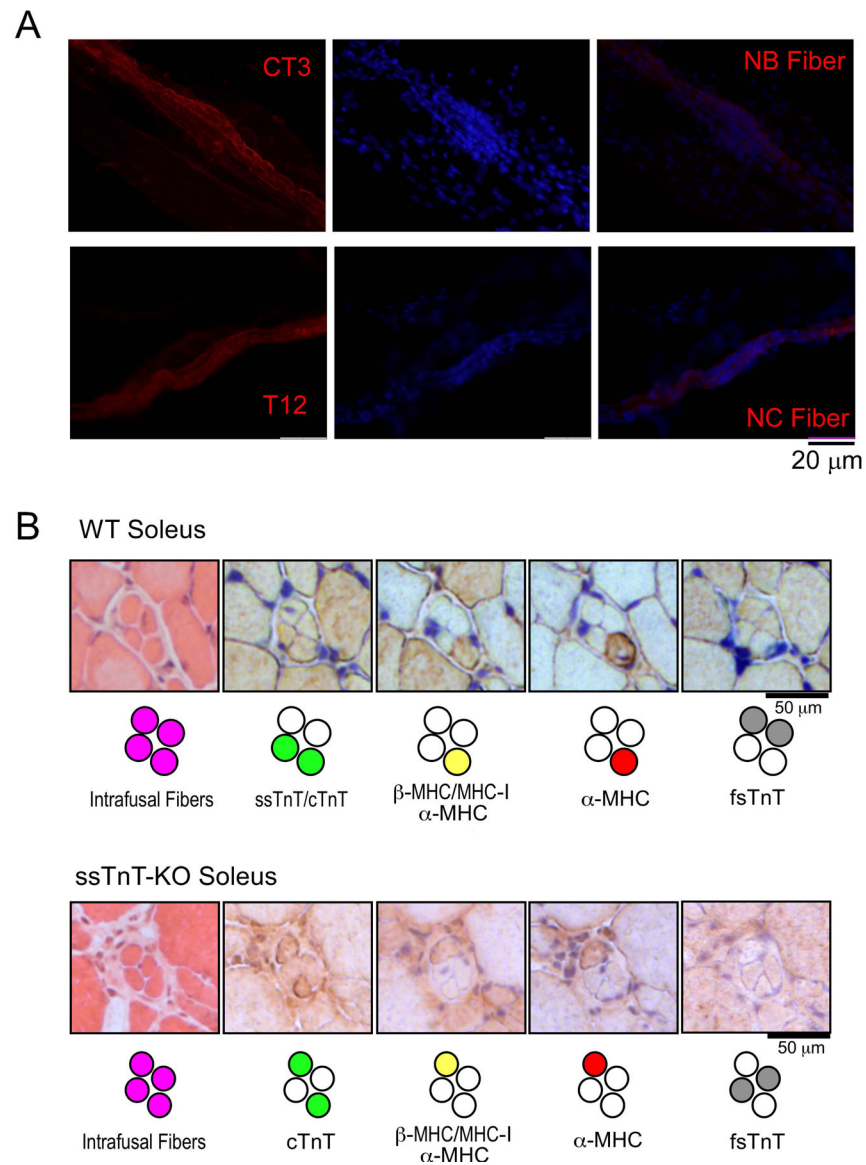


Figure 9. Differential expression of myofilament protein isoforms in nuclear bag and chain fibers.

A. Immunofluorescence staining of isolated spindles from WT mouse soleus muscle revealed that cTnT and ssTnT were expressed in nuclear bag (NB) fibers (stained by mAb CT3) whereas fsTnT was expressed exclusively in nuclear chain (NC) fibers (stained by mAb T12). B. Immunohistochemistry staining showed that the expressions of cTnT/ssTnT and fsTnT were restricted to two of the four intrafusal fibers of WT mouse muscle spindles whereas only one of the two cTnT/ssTnT expressing NB fibers expresses cardiac MHC (upper pane). This pattern was retained in spindles of ssTnT-KO mice except that cTnT was expressed in the NB fibers in the absence of ssTnT (lower panel).